Original Article

Role of the stromal cell derived factor-1/CXC chemokine receptor 4 axis in the invasion and metastasis of lung cancer and mechanism

Yun Zeng[1*], Xinwei Wang[1*], Bijian Yin[1], Guohao Xia[1], Zhengjie Shen[2], Wenzhe Gu[3], Mianhua Wu[2]

[1]Department of Medical Oncology, Jiangsu Cancer Hospital, Jiangsu Institute of Cancer Research, Nanjing Medical University Affiliated Cancer Hospital, Nanjing 210009, China; [2]First Clinical College, Nanjing University of Chinese Medicine, Nanjing 210023, China; [3]Department of Otorhinolaryngology, Zhangjiagang Hospital of Traditional Chinese Medicine, Zhangjiagang 215600, China

Contributions: (I) Conception and design: Y Zeng, X Wang; (II) Administrative support: None; (III) Provision of study materials or patients: None; (IV) Collection and assembly of data: B Yin, G Xia, Z Shen, W Gu, M Wu; (V) Data analysis and interpretation: B Yin, G Xia, Z Shen, W Gu, M Wu; (VI) Manuscript writing: All authors; (VII) Final approval of manuscript: All authors.

*Theses authors contributed equally to this work.

Correspondence to: Yun Zeng. Department of Medical Oncology, Jiangsu Cancer Hospital, Jiangsu Institute of Cancer Research, Nanjing Medical University Affiliated Cancer Hospital, Nanjing 210009, China. Email: zengyunjch@hotmail.com.

Background: Lung cancer is the most common tumor, and has the highest incidence and mortality rates among all malignant tumors. Since stromal cell derived factor-1 (SDF-1) and CXC chemokine receptor 4 (CXCR4) are specific to binding sites, they are more important than other members of the families for tumor invasion and metastasis. We herein aimed to investigate the role of the axis of chemokine SDF-1 and its receptor CXCR4 in the invasion and metastasis of lung cancer.

Methods: Sixty clinical non-small cell lung cancer (NSCLC) tissue samples were collected. The CXCR4 expressions in cancer, paracancerous and normal lung tissues were detected by immunocytochemical assay and PCR. Cells with CXCR4 overexpression (CXCR4-A549) were constructed. After induction with SDF-1, CXCR4-A549 and A549 cells were subjected to *in vitro* chemotaxis and invasion assays. Their proliferation and apoptosis were detected by flow cytometry. The activities of phosphoinositide 3-kinase/protein kinase B (AKT) and mitogen-activated protein kinase/extracellular signal-regulated kinase (ERK)-related signaling pathways were detected by Western blot. The downstream signaling molecules that may be activated by SDF-1/CXCR4 were analyzed. The expressions of vascular endothelial growth factor-C and matrix metalloproteinase-2 were detected by Western blot and PCR. A mouse model was established by subcutaneous inoculation of lung cancer cells. The effects of up-regulated CXCR4 expression on the migration of lung cancer cells *in vitro* and their tumorigenesis and metastasis *in vivo* were assessed.

Results: There was no expression in normal or paracancerous tissues. The expression of CXCR4 mRNA in lung cancer tissues was 83.3% (50/60). The expressions of CXCR4 in lung squamous cell carcinoma and adenocarcinoma were similar (P>0.05). The expression of CXCR4 was 76.9% (10/13) in highly differentiated carcinoma, 82.1% (23/28) in moderately differentiated carcinoma and 84.2% (16/19) in lowly differentiated carcinoma (P>0.05). The expression of CXCR4 was 72.7% (8/11) in TNM stage I patients, 83.9% (26/31) in stage II patients, and 88.9% (16/18) in stage III patients, with significant correlations. After up-regulation of CXCR4, the invasion ability of CXCR4-A549 cells was increased 1.62-fold (P<0.05). ERK and AKT were significantly phosphorylated 30 min after SDF-1 treatment. The tumorigenic rates of six mice inoculated with CXCR4-A549 and A549 cells were both 100%, with the average tumor weights of (4.37±0.96 g) and (3.24±1.16 g) respectively (P<0.05). In the CXCR4-A549 group, metastatic tumors clearly formed in the lungs of 6 mice, but only 2 mice in the A549 group had tumor cell invasion.

Conclusions: SDF-1/CXCR4 played a key role in the invasion and metastasis of lung cancer. The interaction between SDF-1α and CXCR4 activated a series of downstream molecules by activating ERK and AKT.

Keywords: Stromal cell derived factor-1 (SDF-1); CXC chemokine receptor 4 (CXCR4); metastasis; lung cancer

Submitted Mar 27, 2017. Accepted for publication Oct 24, 2017.
doi: 10.21037/jtd.2017.10.138
View this article at: http://dx.doi.org/10.21037/jtd.2017.10.138

Introduction

Lung cancer has the highest incidence and mortality rates among all malignant tumors (1). Tumor metastasis is the main cause for treatment failure and death. This organ-selective metastasis is similar to the migration of inflammatory cells. A variety of inflammatory mediators are of great significance to the onset, progression and metastasis of malignant tumors (2). Chemokines and their receptors initially drive white blood cell migration in the immune system, which participate in various physiological and pathological processes such as lymphatic system development, hematopoiesis, angiogenesis, inflammation, allergic reaction and HIV infection (3). They provide a migration signal for inflammatory cells and play a vital role in cell activation, migration and localization. Many tumor cells can express certain chemokines or receptors in a limited manner, and chemokine-related signaling pathways are no longer regulated, suggesting that chemokines and their receptors are closely related to tumor invasion and metastasis following a mechanism similar to that of inflammatory cell invasion (4).

Chemokine SDF-1 (stromal cell derived factor-1, also known as CXC chemokine ligand 12) and its specific receptor CXC chemokine receptor 4 (CXCR4) interact and constitute a pair of molecules closely related to cell signal transduction, migration and localization, i.e., the SDF-1/CXCR4 axis. This axis plays a key role in inflammatory cell invasion, migration, organ development and other physiological and pathological processes (5). The SDF-1/CXCR4 axis is capable of orientation, driving and localization during the metastasis of breast cancer (6). Moreover, CXCR4 is overexpressed in certain tumor tissues, and can control the invasion of inflammatory cells, regulate tumor angiogenesis, activate the host's specific immune response to tumor cells, stimulate their proliferation in an autocrine or paracrine way, and control their migration through the SDF-1/CXCR4 axis (7). Since SDF-1 and CXCR4 are specific to binding sites, they are more important than other members of the families for tumor invasion and metastasis, also as the focus of this study.

We herein explored the role of SDF-1/CXCR4 in lung cancer invasion and metastasis by both *in vitro* and *in vivo* experiments. The molecular mechanism was explored by up-regulating CXCR4 expression and then detecting changes in the expressions of genes in related signaling pathways and those associated with metastasis. The results provide a valuable evidence for the prevention and treatment of lung cancer metastasis.

Methods

Baseline clinical data

This study has been approved by the ethics committee of Jiangsu Cancer Hospital (No. 20160036), and written consent has been obtained from all patients. Inclusion criteria: non-small cell lung cancer (NSCLC) samples were taken by surgical resection in our hospital from August 2015 to August 2016. The patients receiving neoadjuvant radiotherapy and chemotherapy were excluded. All samples were fixed with 10% formalin, embedded in paraffin, sectioned, HE-stained, and confirmed by pathological examination. Typing and grading were conducted according to the WHO standards, and staging was performed according to the NSCLC P-TNM staging criteria of the Union for International Cancer Control revised in 2015.

Clinical data: sixty NSCLC samples were collected. There were 42 males and 18 females aged between 37 and 72 years old, (59.39±10.21) on average. Pathological data: TNM staging: 16 cases of stage I, 27 cases of stage II, 17 cases of stage III; pathological typing: 36 cases of lung adenocarcinoma and 24 cases of lung squamous cell carcinoma; differentiation degree: 19 cases of high differentiation, 23 cases of moderate differentiation and 18 cases of low differentiation.

Sample collection

All NSCLC samples were dissected immediately after being separated. Tumor issue with active growth was cut along the edge of the tumor, and paracancerous tissue was cut 2 cm

away from the edge. Normal lung tissue was cut 10 cm away from the tumor edge. Then the tissues were cut into blocks with a size of 1 cm × 1 cm × 1cm, packaged in labeled cryogenic vials, put immediately into liquid nitrogen, and then stored in a –80 ℃ refrigerator.

Cells and reagents

Human lung adenocarcinoma cell line A549, human pEGFP-C1 eukaryotic expression plasmid and *Escherichia coli* DH5α strain were purchased from Shanghai Institute of Cell Biology, Chinese Academy of Sciences (China). Mouse anti-human CXCR4 antibody, mouse anti-human β-actin antibody and kits were all purchased from Santa Cruz (USA). Mouse anti-human matrix metalloproteinase-2 (MMP-2), vascular endothelial growth factor-C (VEGF-C), protein kinase B (AKT), phosphorylated AKT (pAKT), extracellular signal-regulated kinase (ERK) and phosphorylated ERK (pERK) antibodies were all purchased from Cell Signaling (USA).

In vitro transfection of A549 cells with pEGFP-C1-CXCR4

The culture medium was replaced with serum-free DMEM for transfection. The cells were divided into Groups A, B and C which were normal A549 cells without transfection, A549 cells transfected with empty vector pEGFP-C1 and A549 cells transfected by pEGFP-C1-CXCR4 respectively.

Transfection process: solution 1:250 μL of serum-free DMEM (Group B was added with solution 1 and empty vector pEGFP-C1, and Group C was added with solution 1 and 3 μg of EGFP-C1-CXCR4 plasmid); solution 2:250 μL of serum-free DMEM was added with 6 μL of lipofectamine™ 2,000 liposomes. Solutions 1 and 2 were mixed and placed at room temperature for 30 min. Groups B and C were added with corresponding mixture, and placed in a CO_2 incubator for 4 h. Then the medium was replaced with DMEM/F12 medium containing 15% NCS to further culture the cells for 24 h. Then DMEM/F12 screening medium containing G418 and 15% NCS was used instead to continue culture.

Immunohistochemical assay

All samples were fixed with 10% formalin, embedded with paraffin, and sectioned continuously into 5 μm-thicks. The sections were placed into an oven at 60 ℃ overnight, then taken out, sequentially put into xylene I for 20 min, xylene II for 20 min, 95% ethanol I for 5 min and 95% ethanol II for 5 min, washed with tap water, and deparaffinized. After 5% H_2O_2 was used to inactivate endogenous peroxidase, the sections were placed at room temperature for 30 min, and washed with PBS 3 times (3 min each time). Antigen retrieval: the sections were placed in a container with citrate buffer (0.01 M, pH 6), heated in a microwave oven (450 W, the temperature kept at 95 to 100 ℃) for 10 min, taken out, and cooled naturally at room temperature. Then the sections were rinsed with PBS 3 times (3 min each time), dropwise added with 10% goat serum for blocking and incubated at 37 ℃ for 10 min, after which excess liquid was removed. They were thereafter added with monoclonal antibody and incubated at 37 ℃ for 1 h and then at 4 ℃ overnight. Subsequently, the sections were rewarmed at 37 ℃ for 1 h, rinsed with PBS 3 times (3 min each time), added with secondary antibody for reaction at 37 ℃ for 1 h, and developed with 0.05% DAB +0.03% H_2O_2. The reaction was then terminated, and the sections were counterstained mildly with hematoxylin, dehydrated, transparentized and mounted.

Immunohistochemical assay was conducted with the double-blinded method by experienced personnel in order to guarantee the objectiveness of observations. Scoring for immunohistochemical assay: according to the semi-quantitative integration method, five high-power visual fields were randomly selected for each case (magnification: ×400). Scoring for percentage of positive cells: ≤5%, 0 point; 6–25%, 1 point; 26–50%, 2 points; 51–75%, 3 points; >75%, 4 points. Scoring for positive intensity: colorless, 0 point; yellow, 1 point; brownish yellow, 2 points; brown, 3 points. Then the scores of positive cell percentage and positive intensity were multiplied: 0 point, negative (–); 1–2 points, weakly positive (+); 3–5 points, moderately positive (++); 6–8 points, strongly positive (+++).

Real-time PCR

About 100 mg of tissue samples were taken out from the –80 ℃ refrigerator, placed in a mortar, and crushed in the presence of liquid nitrogen. After liquid nitrogen was dried, the samples were immediately added with 1 mL of Trizol, continuously ground until they completely turned into liquid, and then transferred into 1.5 mL centrifuge tubes. RNA was extracted from cells, and its expression was detected using real-time PCR kit. Electrophoresis was performed on 1.5% agarose gel, and the results were observed and scanned by Image-Pro Plus image analyzer.

Western blot

Cells were collected by digestion and centrifugation, resuspended by adding RIPA (50 mM pH 7.5 Tris-HCl, 150 mM NaCl, 1% NP-40, 0.5% sodium deoxycholate, 0.1% SDS), ultrasonicated, and centrifuged at 12,000 rpm and 4 ℃ for 10 min. The total protein concentration was measured according to the BCA kit's instructions. Each sample (50 μg) was taken for SDS-PAGE. Afterwards, the proteins were transferred to a nitrocellulose membrane that was then blocked with 5% skimmed milk at room temperature for 1 h and incubated with primary antibody at 4 ℃ overnight. After being washed, the membrane was further incubated with secondary antibody at 37 ℃ for 1 h. After ECL development, scanning was conducted, and the relative expression of protein was corrected with internal reference and analyzed by Quantity-One software.

Chemotaxis assay

RPMI 1,640 medium (500 μL) containing 5% BSA was added to the lower 24-well chemotaxis chamber that was thereafter covered with polycarbonate membrane (pore size: 8 μm) which had been treated with fibronectin (5.0 μg/mL). The upper chamber was added with 400 μL of single cell suspension (1×10^5) made by serum-free RPMI 1,640 medium and incubated in a 5% CO_2 incubator at 37 ℃ for 12 h. Negative control: Only RPMI 1,640 medium containing 0.5% BSA was added to the lower chamber. Three replicate wells were set for each group. The chemotaxis membrane was fixed with methanol and then subjected to HE staining. The cells in at least 5 visual fields (×100) were counted under an optical microscope, and the mean in each visual field was reported.

Invasion assay

The supernatant of chemotaxis assay (500 μL) containing SDF-1α (RPMI 1,640 medium +0.5% BSA +100 ng/mL SDF-1α) was added to the lower 24-well chemotaxis chamber that was thereafter coated with polycarbonate membrane which had been coated with Matrigel basement membrane (pore size: 8 μm). The upper chamber was added with 400 μL of single cell suspension (1×10^5) (RPMI 1,640 medium +0.5% BSA) and incubated in a 5% CO_2 incubator at 37 ℃ for 24 h. Cells were incubated with anti-human CXCR4 antibody (50 pg/mL) for 30 min at 37 ℃, and then the invasion assay was performed. Negative control: only RPMI 1,640 medium containing 0.5% BSA was added to the lower chamber. Three replicate wells were set for each group. The chemotaxis membrane was fixed with methanol and then subjected to HE staining. The cells in at least 5 visual fields (×100) were counted under an optical microscope, and the mean in each visual field was reported.

Detection of cell apoptosis by flow cytometry

The adherent cells in a culture flask were digested using 0.25% trypsin + EDTA, and then the cell suspension was transferred to a centrifuge tube, with the number of about 2×10^6. The cells were washed with 3 mL of PBS once and centrifuged at 1,000 rpm for 2 min. After PBS was discarded, the cells were added with 750 mL/L pre-cooled ethanol and fixed at 4 ℃ for 24–48 h. The fixing solution was discarded by centrifugation, and the cells were resuspended with 3 mL of PBS for 5 min and centrifuged at 1,000 rpm for 5 min to discard PBS. The cell concentration was adjusted to 1×10^6/mL. Then the cells were added with RNase to the final concentration of 1 g/L, and put in water bath at 37 ℃ for 30 min. The cell aggregate was removed by 350-mesh nylon filter membrane. Apoptosis detection: The cells were stained by 1 mL of PI and FITC-annexin V solution and kept in dark at 4 ℃ for 30 min. The results were analyzed using Cell quest software. B1 quadrant represents apoptotic cells due to mechanical damage, B2 represents cells at the late apoptosis stage, B3 represents viable cells, and B4 represents cells at the early apoptosis stage.

Establishment of a mouse model bearing spontaneously metastasized human lung cancer cells

CXCR4-A549 cells and A549 cells in the exponential growth phase were collected. The rate of viable cells was confirmed to exceed 90% by counting and 0.1% trypan blue staining. After centrifugation at 1,000 rpm for 5 min, the supernatant was removed. The cells were resuspended with PBS, pipetted into a single cell suspension, and inoculated subcutaneously into the hip joint of nude mice at 5×10^6/400 μL, 6 mice for each group. Samples were collected 10 weeks later, and then the tumors and lungs were separated *in situ*, fixed with 10% formalin, embedded with paraffin, sectioned into 5 μm-thicks, and subjected to HE staining to observe metastasis.

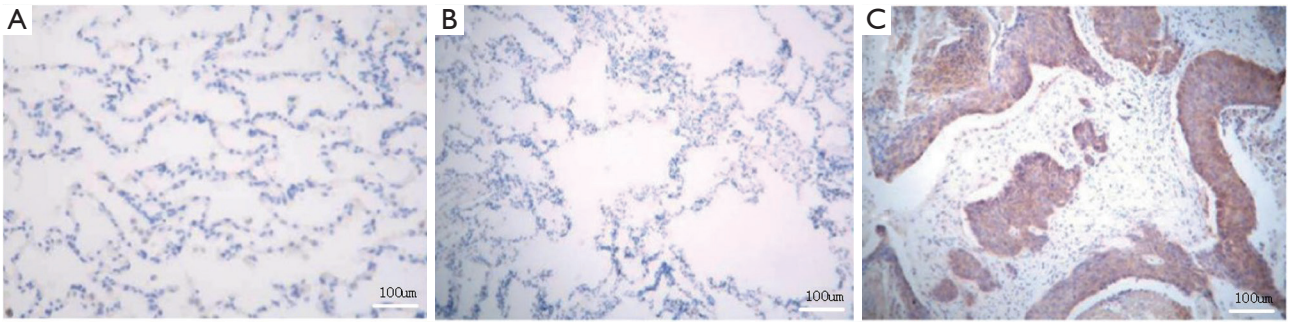

Figure 1 CXCR4 expressions in (A) normal, (B) paracancerous and (C) NSCLC tissues. Immunohistochemical staining was used. CXCR4, CXC chemokine receptor 4; NSCLC, non-small cell lung cancer.

Table 1 CXCR4 expressions in NSCLC tissues (n=60)

Type	CXCR4				P
	–	+	++	+++	
NSCLC tissue	10	24	21	5	0.001
Paracancerous tissue	0	0	0	0	
Normal tissue	0	0	0	0	

–, negative; +, weakly positive; ++, moderately positive; +++, strongly positive. CXCR4, CXC chemokine receptor 4; NSCLC, non-small cell lung cancer.

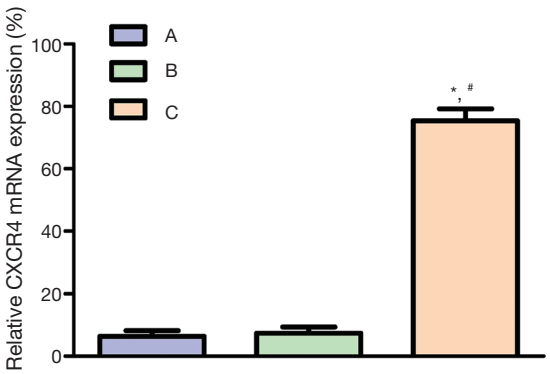

Figure 2 CXCR4 mRNA expressions in (A) normal, (B) paracancerous and (C) NSCLC tissues. *, comparison between B and A, P<0.05; #, comparison between B and C, P<0.05. CXCR4, CXC chemokine receptor 4; NSCLC, non-small cell lung cancer.

Statistical analysis

Each experiment was independently performed in triplicate. All data were analyzed by SPSS22.0 and expressed as mean ± standard deviation. Comparisons between two groups were conducted by the test, and those between multiple groups were carried out by one-way analysis of variance. P<0.05 was considered statistically significant.

Results

Clinical sample detection results

CXCR4 expressions in NSCLC tissues

Immunohistochemical assay showed that CXCR4 was mainly expressed in the cell membrane and cytoplasm. There was no expression in normal or paracancerous tissues (*Figure 1A*,*B*), and the CXCR4 positive rate of NSCLC tissues was 83.3% (50/60) (*Figure 1C*). The CXCR4 expression levels of NSCLC and normal tissues were significantly different (P=0.001) (*Table 1*).

CXCR4 mRNA expressions in NSCLC tissues

The specific band of CXCR4 mRNA was at 260 bp. The expression rates of CXCR4 mRNA in NSCLC, paracancerous and normal tissues were 83.3% (50/60), 38.3% (23/60) and 31.7% (19/60) respectively. The rate of NSCLC tissues was significantly higher than those of paracancerous and tissues (P=0.032), but the latter two had similar results (P>0.05) (*Figure 2*).

Correlations between CXCR4 expression in NSCLC tissues and clinical pathological characteristics

To further explore the correlations between CXCR4 expression and the invasion, metastasis and prognosis of NSCLC, all cases were grouped according to pathological type, differentiation degree and TNM stage.

Correlation between CXCR4 expression and pathological type

The expression rates of CXCR4 in squamous cell carcinoma

Table 2 Correlation between CXCR4 expression and pathological type (n=60)

Pathological type	Case No.	CXCR4				P
		–	+	++	+++	
Squamous cell carcinoma	29	6	11	10	2	>0.05
Adenocarcinoma	31	4	13	11	3	
Total	60	10	24	21	5	

–, negative; +, weakly positive; ++, moderately positive; +++, strongly positive. CXCR4, CXC chemokine receptor 4.

Table 3 Correlation between CXCR4 and degree of tumor differentiation (n=60)

Differentiation degree	Case No.	CXCR4				P
		–	+	++	+++	
High	13	3	4	5	1	>0.05
Moderate	28	5	10	10	3	
Low	19	2	10	6	1	
Total	60	10	24	21	5	

–, negative; +, weakly positive; ++, moderately positive; +++, strongly positive. CXCR4, CXC chemokine receptor 4.

Table 4 Correlation between CXCR4 expression and TNM stage (n=60)

TNM stage	Case No.	CXCR4				P
		–	+	++	+++	
I	11	3	5	2	1	0.032
II	31	5	15	10	1	
III	18	2	4	9	3	
Total	60	10	24	21	5	

–, negative; +, weakly positive; ++, moderately positive; +++, strongly positive. CXCR4, CXC chemokine receptor 4.

and adenocarcinoma were 79.3% (23/29) and 87.1% (27/31) respectively, without a significant difference (P>0.05) (*Table 2*).

Correlation between CXCR4 and degree of tumor differentiation

The expression rate of CXCR4 was 76.9% (10/13) in highly differentiated carcinoma, 82.1% (23/28) in moderately differentiated carcinoma and 84.2% (16/19) in lowly differentiated carcinoma, without significant differences (P>0.05) (*Table 3*). Since CXCR4 expression increased with decreasing differentiation degree, the expression showed trend towards negative association with malignancy degree.

Correlation between CXCR4 expression and TNM stage

The expression rate of CXCR4 was 72.7% (8/11) in TNM stage I patients, 83.9% (26/31) in stage II patients, and 88.9% (16/18) in stage III patients, which showed significant correlations (P=0.032) (*Table 4*). Clearly, the incidence of CXCR4 positive samples was higher at a later TNM stage.

Correlations between CXCR4 and metastasis-related gene expressions

To explore whether CXCR4 interacted with VEGF and MMPs to promote NSCLC invasion and metastasis, we detected the expression levels of VEGF-C and MMP-3 in NSCLC tissues by immunohistochemical assay.

VEGF-C expression in NSCLC tissues

VEGF-C expression in NSCLC tissues is presented in *Figure 3A*. VEGF-C was not expressed in paracancerous or normal tissues, but the incidence of positive samples in NSCLC tissue was 65.0% (39/60) (*Table 5*). The expressions of CXCR4 and VEGF-C were positively correlated (r=0.729, P=0.047) (*Table 6*).

MMP-2 expression in NSCLC tissues

MMP-2 expression in NSCLC tissues is exhibited in *Figure 3B*. MMP-2 was not expressed in paracancerous or normal tissues, whereas the incidence of positive samples in NSCLC tissue was 60.0% (36/60) (*Table 5*). The expressions of CXCR4 and MMP-2 were positively correlated (r=0.734, P=0.039) (*Table 7*).

In vitro experimental results

Identification of cells stably transfected with CXCR4

A549 cells did not express EGFP, but this protein was highly expressed in those transfected with pEGFP-C1-CXCR4 plasmid (*Figure 4A*). Western blot showed that the CXCR4 protein expression of CXCR4-A549 cells was significantly higher than that of untransfected CXCR4 cells (*Figure 4B,C*), indicating that cells stably transfected with CXCR4 had been successfully constructed.

Effects of CXCR4 on *in vitro* invasion of lung cancer cells

To study the relationship between CXCR4 and the

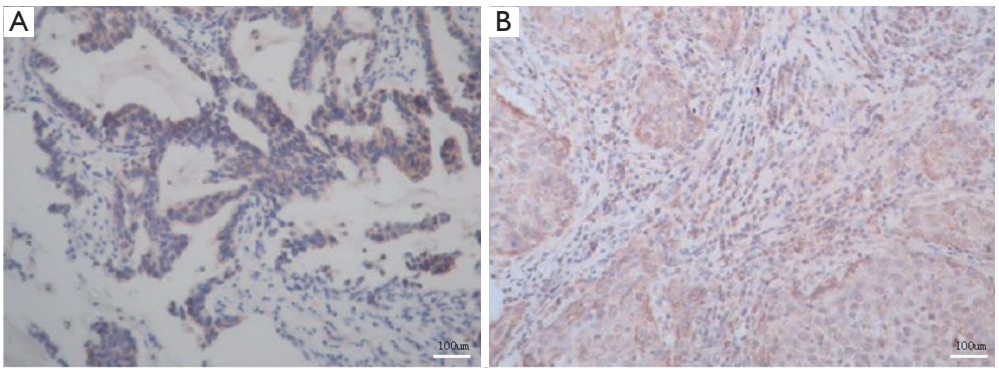

Figure 3 VEGF-C (A) and MMP-2 (B) expressions in NSCLC tissues. Immunohistochemical staining was used. VEGF-C, vascular endothelial growth factor-C; MMP-2, matrix metalloproteinase-2; NSCLC, non-small cell lung cancer.

Table 5 CXCR4, VEGF-C and MMP-2 expressions in NSCLC tissues (n=60)

Type	Expression level				Total
	–	+	++	+++	
CXCR4	10	24	21	5	50 (83.3%)
VEGF-C	21	26	12	1	39 (65.0%)
MMP-2	24	18	14	4	36 (60.0%)

–, negative; +, weakly positive; ++, moderately positive; +++, strongly positive. CXCR4, CXC chemokine receptor 4; VEGF-C, vascular endothelial growth factor-C; MMP-2, matrix metalloproteinase-2; NSCLC, non-small cell lung cancer.

Table 6 Correlation between VEGF-C and CXCR4 expressions

VEGF-C	CXCR4				
	– (n=10)	+ (n=24)	++ (n=21)	+++ (n=5)	
– (n=21)	10	10	1	0	r=0.729
+ (n=26)	0	13	10	3	P=0.047
++ (n=12)	0	1	10	1	
+++ (n=1)	0	0	0	1	

–, negative; +, weakly positive; ++, moderately positive; +++, strongly positive. VEGF-C, vascular endothelial growth factor-C; CXCR4, CXC chemokine receptor 4.

Table 7 Correlation between MMP-2 and CXCR4 expressions

MMP-2	CXCR4				
	– (n=10)	+ (n=24)	++ (n=21)	+++ (n=5)	
– (n=24)	9	10	5	0	r=0.729
+ (n=18)	1	12	5	0	P=0.047
++ (n=14)	0	2	10	2	
+++ (n=4)	0	0	1	3	

–, Negative; +, weakly positive; ++, moderately positive; +++, strongly positive. MMP-2, matrix metalloproteinase-2; CXCR4, CXC chemokine receptor 4.

metastatic potential of lung cancer cells, we first study the effects of up-regulated CXCR4 expression on *in vitro* invasion ability. The number of invasive CXCR4-A549 cells was (45.5±2.5), and that of invasive A549 cells was (28.0±2.1) (*Figure 5A*). Transwell assay showed that after up-regulation of CXCR4, the invasion ability of CXCR4-A549 cells was increased 1.62-fold (P<0.05). After addition of CXCR4 neutralizing antibody, the numbers of invasive CXCR4-A549 cells and invasive A549 cells were (35.1±2.6) and (17.6±2.4) respectively (*Figure 5B*). The invasion capacities of the two groups both decreased significantly (P<0.05). Therefore, the *in vitro* invasion ability of lung cancer cells was affected by regulating CXCR4 expression during metastasis.

Effects of SDF-1/CXCR4 on *in vitro* chemotaxis and invasion of lung cancer cells

After induction with 100 ng/mL SDF-1α, the numbers of migrating and invasive CXCR4-A549 cells were (75.5±2.1) and (74.0±2.3) respectively, and those of migrating and invasive A549 cells were (34.6±1.4) and (32.1±1.1) respectively (*Figure 6A,B*). The migration and invasive abilities of CXCR4-A549 cells significantly exceeded those of A549 cells (P<0.05). However, the capacities of both groups significantly reduced after addition of CXCR4

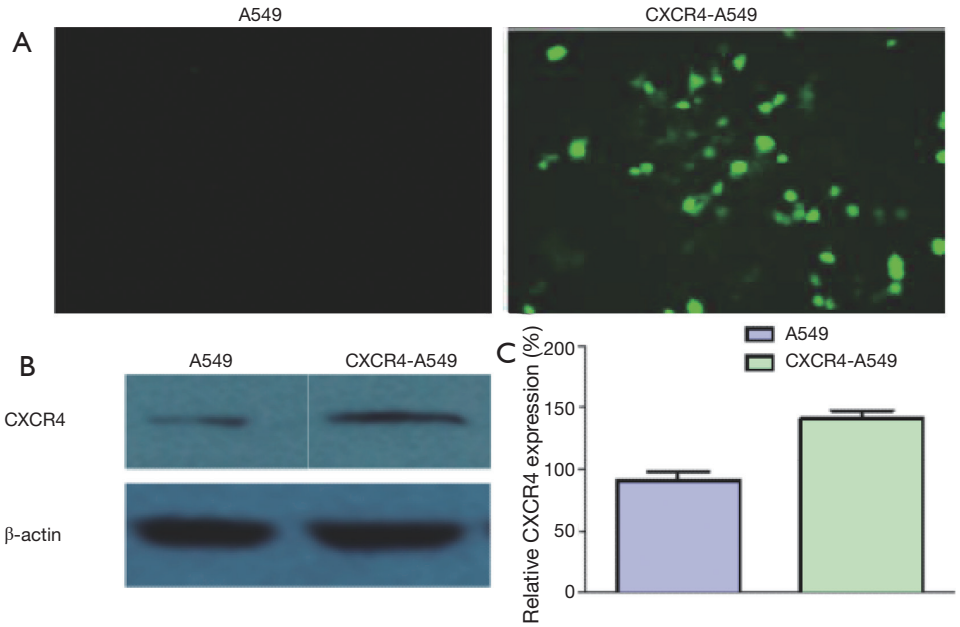

Figure 4 CXCR4 protein expressions detected by (A) green fluorescence and (B) Western blot; (C) histogram for Western blot results. CXCR4, CXC chemokine receptor 4.

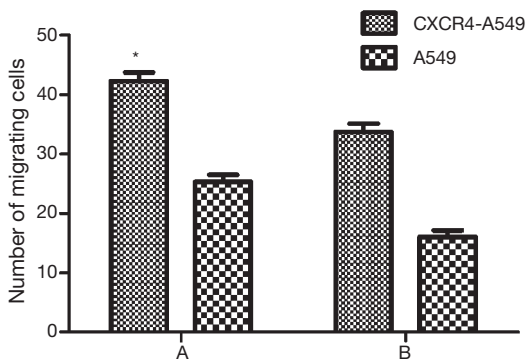

Figure 5 Effects of CXCR4 on *in vitro* invasion ability of lung cancer cells (A) before and (B) after addition of CXCR4 neutralizing antibody. *, comparison between CXCR4-A549 and A549 cells, P<0.05. CXCR4, CXC chemokine receptor 4.

neutralizing antibody (P<0.05) (*Figure 6A,B*). Thus, SDF-1α-induced chemotaxis and invasion were mediated by the specificity of CXCR4.

Cell apoptosis results detected by flow cytometry

Flow cytometry showed that the apoptotic rates of CXCR4-A549 (0.4%) and A549 cells (0.8%) were similar (P>0.05) (*Figure 7*).

Regulatory effects of SDF-1/CXCR4 on MMP-2 and VEGF-C expressions

In clinical NSCLC tissues, the expression of CXCR4 was correlated with those of MMP-2 and VEGF-C. We first constructed a cell line overexpressing CXCR4 and performed Western blot. The protein levels of VEGF-C and MMP-2 significantly increased in CXCR4-A549 cells, and such effect was further enhanced by SDF-1α stimulation (P<0.05) (*Figure 8*). Accordingly, the interaction between SDF-1 and CXCR4 regulated MMP-2 and VEGF-C expressions in lung cancer cells.

Inducing effects of SDF-1 on phosphorylation of ERK and AKT

CXCR4 is a G protein–coupled receptor, so its possible signaling pathways are phosphoinositide 3-kinase (PI3K)/AKT and mitogen-activated protein kinase (MAPK)/ERK. As a result, we detected the phosphorylation of ERK and AKT in the presence of SDF-1α. CXCR4-A549 cells were cultured in serum-free medium for 12 h, added 100 ng/mL SDF-1α and collected at 0, 15 and 30 min respectively for Western blot. ERK and AKT were phosphorylated 15 and 30 min after SDF-1α treatment, which was more obvious at 30 min (*Figure 9*). Hence, the interaction between SDF-1α and CXCR4 activated a series of downstream molecules by

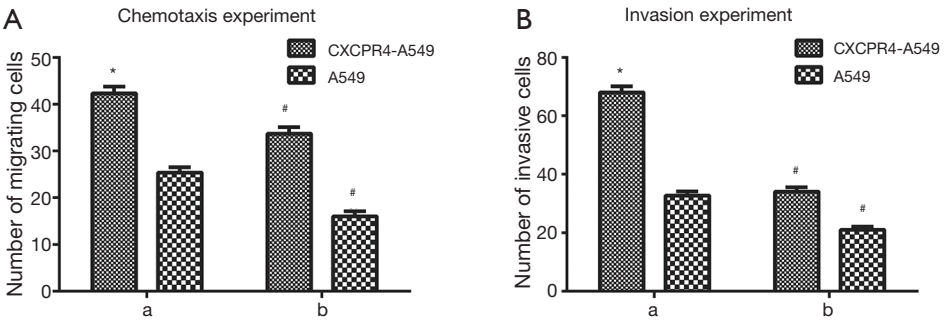

Figure 6 Effects of SDF-1/CXCR4 on chemotaxis and invasion of lung cancer cells (A) before and (B) after addition of CXCR4 neutralizing antibody. *, comparison between CXCR4-A549 and A549 cells, P<0.05; #, comparison between CXCR4-A549 and A549 cells after addition of CXCR4 and those before addition, P<0.05. SDF-1, stromal cell derived factor-1; CXCR4, CXC chemokine receptor 4.

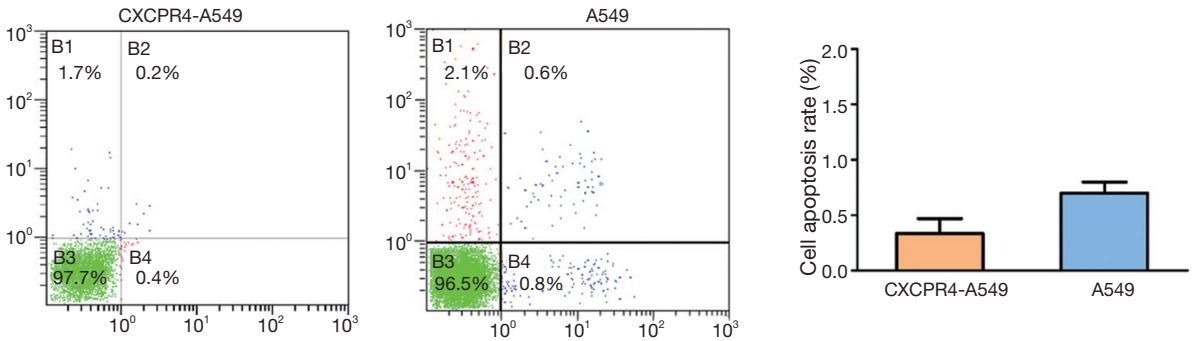

Figure 7 The apoptotic rates of CXCR4-A549 (0.4%) and A549 cells (0.8%) were similar (P>0.05). CXCR4, CXC chemokine receptor 4.

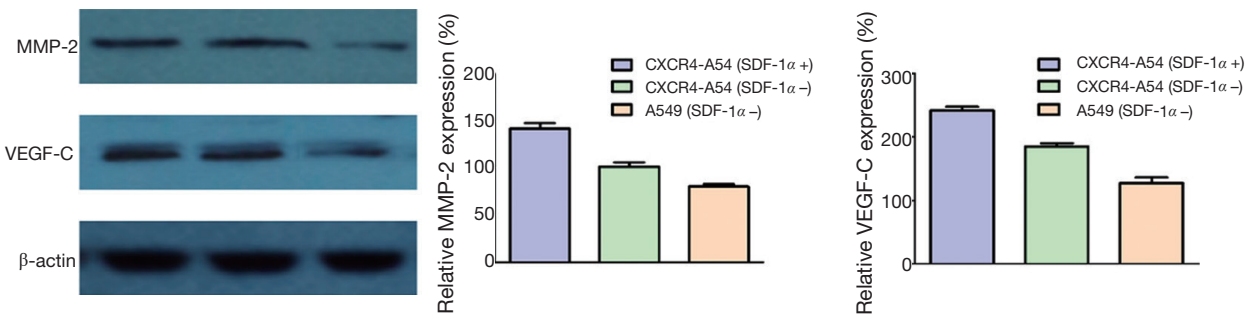

Figure 8 MMP-2 and VEGF-C expressions detected by Western blot. MMP-2, matrix metalloproteinase-2; VEGF-C, vascular endothelial growth factor-C.

activating ERK and AKT, finally mediating cell migration.

In vivo experimental results

In the *in vivo* experiment, the tumorigenic rates of six mice inoculated with CXCR4-A549 and A549 cells were both 100%, with the average tumor weights of (4.37±0.96 g) and (3.24±1.16 g) respectively, between which the difference was significantly significant (P<0.05) (*Figure 10A*). In the CXCR4-A549 group, metastatic tumors clearly formed in the lungs of 6 mice (*Figure 10A,B*), but only 2 mice in the A549 group had tumor cell invasion, without apparent formation of metastatic tumor (*Figure 10C*). The results suggested that

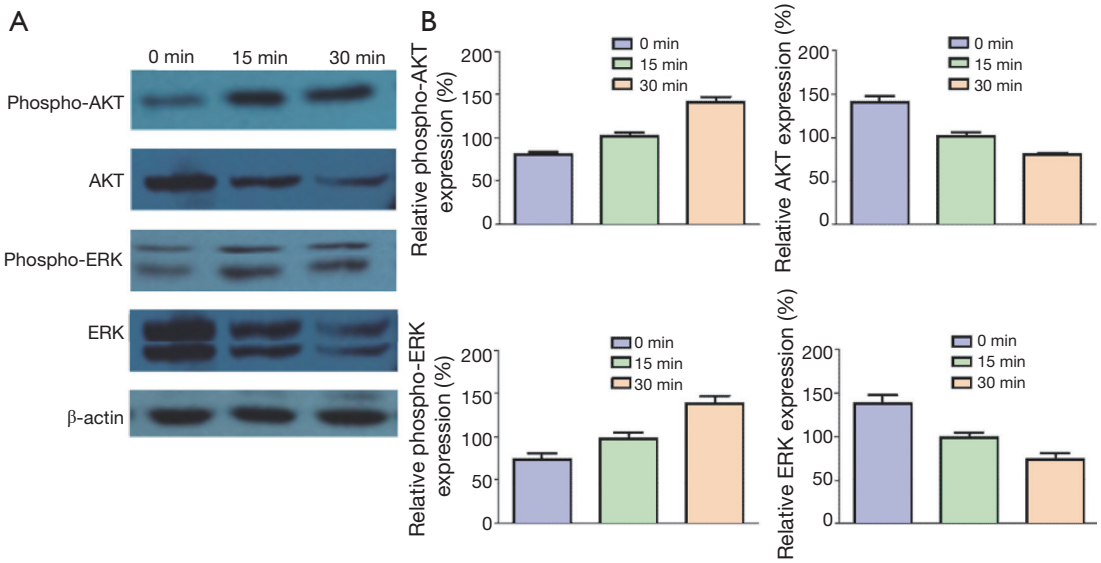

Figure 9 SDF-1-induced phosphorylation of ERK and AKT. (A) Western blot results; (B) histograms for Western blot results. ERK, extracellular signal-regulated kinase; ART, protein kinase B.

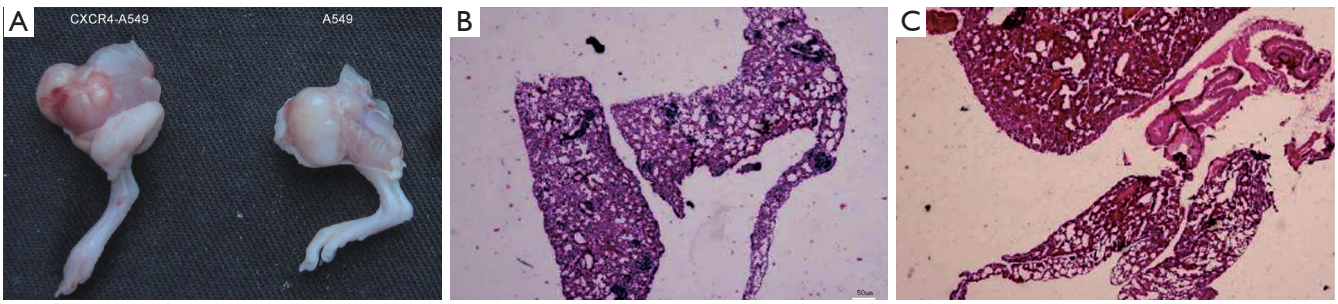

Figure 10 Effects of CXCR4 on *in vivo* invasion and metastasis of lung cancer cells. (A) Primary tumors formed in two groups after cell inoculation; (B) invasion of tumor cells in the lung tissue of A549 group; (C) formation of metastatic tumor in the lung tissue of CXCR4-A549 group. HE staining was used. CXCR4-A549 group contained 13 tumor foci in lungs, while A549 group contained none. CXCR4, CXC chemokine receptor 4.

up-regulating CXCR4 expression promoted the *in vivo* invasion and metastasis of lung cancer cells.

Discussion

The interaction of SDF-1 with its receptor CXCR4 constitutes a pair of molecules, i.e., the SDF-1/CXCR4 axis, which is closely related to intracellular signaling transduction and cell migration (8). This axis plays an important role in inflammatory cell infiltration, migration and organ development (9). CXCR4 is expressed in many cancers, such as breast cancer, prostate cancer, pancreatic cancer, colon cancer, ovarian cancer, neuroblastoma and glioma (10,11). We detected the expressions of CXCR4 in 60 cases of NSCLC tissues by immunohistochemical assay. CXCR4 was expressed in the cell membrane and cytoplasm of lung cancer tissues. Compared with paracancerous and normal lung tissues, both squamous cell lung carcinoma and lung adenocarcinoma had the CXCR4 expression rates of 83.3% (50/60), indicating that CXCR4 expression was a common characteristic of NSCLC.

Besides, CXCR4 expression has been related to tumor cell malignancy and prognosis. In refractory metastatic prostate cancer, CXCR4 is an aggressive phenotype (12).

CXCR4 mRNA expression is up-regulated in invasive and advanced bladder cancer tissues, but the expression is low in superficial bladder cancer (13). In this study, although the expression level of CXCR4 increased with decreasing degree of cell differentiation, there was no significant difference. Thus, CXCR4 expression was not closely related to the differentiation of lung cancer cells, and tumor metastasis may only be associated with the amount of CXCR4 in local cells. The postulation still needs further validation. The expressions of CXCR4 differ significantly in NSCLC patients at different TNM stages (14). In particular, the expression of CXCR4 is significantly higher at stages II and III lung cancer with lymphatic metastasis and local infiltration than that at stage I (15), suggesting that such expression is closely associated with the invasion and metastasis of tumor cells, probably as one of the indices for determining the prognosis of NSCLC.

VEGF is the most important stimulating factor for tumor neovascularization, and MMPs are the dominant basement membrane-degrading proteases secreted by tumor cells (16). The expressions of VEGF and MMPs are also closely related to tumor invasion and metastasis (17). VEGF-C can promote tumor neovascularization and also function as a lymphangiogenic factor. Additionally, Fukunaga *et al.* (18) reported that the SDF-1/CXCR4 system was associated with VEGF-C, as a marker for lymphangiogenesis. Nevertheless, the relationship between them in lung cancer has seldom been referred. Therefore, we herein selected VEGF-C as the research objective. In this study, the expression rate of VEGF-C in NSCLC tissues was 65.0% (39/60). Of all 60 specimens, 27 had expressions of both CXCR4 and VEGF-C. Accordingly, SDF-1/CXCR4 not only promoted tumor angiogenesis, but may also exert synergistic effects with other pro-angiogenic factors. MMP-2 is a crucial member of the MMPs family and can degrade a variety of extracellular matrices. In human hepatocellular carcinoma cells, SDF-1 can activate MMP-2, leading to enhanced migration and invasion (19). In cervical cancer, SDF-1 not only increases the mRNA level of MMP-2, but also enhances its activity (20). The expression of MMP-2 in NSCLC tissues reached 60.0% (36/60) herein, indicating that high expression of CXCR4 elevated MMP-2 expression in lung cancer to facilitate invasion and metastasis.

Moreover, we verified that the expression of CXCR4 in lung cancer was correlated with clinical TNM stage, typified by increased positive expression in metastatic lung cancer. Afterwards, we constructed a lung cancer cell line stably expressing CXCR4, and up-regulated its CXCR4 expression level to evaluate the effects of SDF-1/CXCR4 on the metastatic potential. The difference between CXCR4 expressions was related to the metastatic potential of lung cancer cells. Up-regulating CXCR4 expression significantly affected the metastatic ability of lung cancer cells *in vitro* and *in vivo*, so the invasion and metastasis of lung cancer may be induced by the interaction between SDF-1 and CXCR4. Cell chemotaxis refers to the directional movement of cells towards chemokines with higher chemotactic concentrations (21). After binding SDF-1, the G protein α subunit of CXCR4 can bind GTP, and the β and γ subunits dissociate to form a dimer, triggering a series of intracellular signaling transductions, cell activation and chemotaxis, and directional cell migration to tissues with higher chemokine concentrations (22). Tumor cells must invade the basement membrane after detachment from primary tumor. Therefore, migration ability is one of the indices for evaluating the *in vitro* metastatic potential of tumor cells, for which the chemotaxis experiment is the optimum strategy (23). Our results showed that the numbers of migrating CXCR4-A549 and A549 cells significantly increased owing to chemotaxis of SDF-1α. After addition of CXCR4 neutralizing antibody, the migration capacities of the two groups significantly decreased, indicating that SDF-1α/CXCR4 specifically affected the migration ability of lung cancer cells. Since the number of migrating cells in the CXCR4-A549 group was significantly higher than that of the A549 group ($P<0.05$), CXCR4 overexpression promoted the migration of lung cancer cells. The main component of endothelial cell basement membrane is collagen, and tumor cells can secrete a variety of proteases to degrade the basement membrane and to allow tumor cell invasion. In this study, due to chemotaxis of SDF-1, the *in vitro* invasion ability of CXCR4-A549 cells was increased 1.62-fold ($P<0.05$) compared with that of the control group. Similarly, after addition of CXCR4 neutralizing antibody, the invasion capacities of both groups decreased ($P<0.05$), indicating that the *in vitro* invasion ability of lung cancer cells was significantly enhanced by up-regulating CXCR4 expression.

The SDF-1/CXCR4 axis participates in lung cancer metastasis probably by regulating tumor neovascularization, basement membrane degradation, cell proliferation, apoptosis, migration, adhesion, selective metastasis to specific organs, etc. (24). The influence of SDF-1 on cell proliferation remains controversial, but the SDF-1/CXCR4 signaling pathway indeed stimulates the proliferation of prostate cancer, glioma, astrocytoma and ovarian epithelial

carcinoma cells (25). We herein observed that the apoptotic rate of CXCR4-A549 cells decreased in the presence of SDF-1, revealing that SDF-1/CXCR4 facilitated the proliferation of tumor cells, but there was no significant difference between the two groups. We thus postulated that SDF-1/CXCR4 promoted metastasis not mainly by regulating the proliferation of lung cancer cells.

After binding of CXCR4 to SDF-1, PI3K and AKT in the cytoplasm are further activated. The activity of AKT is enhanced in many types pf malignant tumors to participate in proliferation, angiogenesis and migration (26). We detected the AKT and pAKT activities of the PI3K kinase pathway in lung cancer cells by Western blot, and found that SDF-1 induced the phosphorylation of AKT. Hence, the interaction between SDF-1 and CXCR4 may activate the PI3K/AKT pathway, so the downstream molecules are activated to participate in the invasion and migration of lung cancer cells.

ERKs are main members of the MAPK family. ERK signal, as the central part of signaling transduction pathway, is involved in the regulation of cytoskeleton, cell growth and differentiation (27). After binding CXCR4 on the surface of T cells, SDF-1 can mediate cell chemotaxis and migration by activating ERK molecule in the MAPK pathway (28). In this study, given that SDF-1 induced activation of the ERK pathway, manifested as ERK phosphorylation, the interaction between SDF-1 and CXCR4 may activate the downstream molecules to participate in the invasion and migration of lung cancer cells by activating MAPK/ERK. After nude mice were subcutaneously inoculated with CXCR4-A549 cells, primary tumor formed at the inoculation site, and multiple metastatic foci appeared in the lung. For the control group inoculated with A549 cells, although primary tumor formed in the hip, there were no metastatic foci in the lung. Homology analysis has verified that the amino acid homology of SDF-1 between human and mouse reached 99% (29), so SDF-1 may be involved in the directional homing/metastasis of human lung cancer cells in this model.

Conclusions

In summary, the correlation between SDF-1/CXCR4 and lung cancer was analyzed by both *in vitro* and *in vivo* experiments. SDF-1/CXCR4 played a key role in the invasion and metastasis of lung cancer. The interaction between SDF-1α and CXCR4 activated a series of downstream molecules by activating ERK and AKT. The findings provide a valuable reference for further studies on lung cancer metastasis as well as clinical diagnosis and treatment.

Acknowledgements

None.

Footnote

Conflicts of Interest: The authors have no conflicts of interest to declare.

Ethical Statement: This study has been approved by the ethics committee of Jiangsu Cancer Hospital (No. 20160036), and written consent has been obtained from all patients.

References

1. Rafiemanesh H, Mehtarpour M, Khani F, et al. Epidemiology, incidence and mortality of lung cancer and their relationship with the development index in the world. J Thorac Dis 2016;8:1094-102.
2. Bazzani L, Donnini S, Finetti F, et al. PGE2/EP3/SRC signaling induces EGFR nuclear translocation and growth through EGFR ligands release in lung adenocarcinoma cells. Oncotarget 2017;8:31270-87.
3. Ozawa PM, Ariza CB, Ishibashi CM, et al. Role of CXCL12 and CXCR4 in normal cerebellar development and medulloblastoma. Int J Cancer 2016;138:10-3.
4. Han KQ, He XQ, Ma MY, et al. Inflammatory microenvironment and expression of chemokines in hepatocellular carcinoma. World J Gastroenterol 2015;21:4864-74.
5. Yu N, Zhang Z, Chen P, et al. Tetramethylpyrazine (TMP), an active ingredient of Chinese herb medicine chuanxiong, attenuates the degeneration of trabecular meshwork through SDF-1/CXCR4 axis. PloS One 2015;10:e0133055.
6. Jin F, Brockmeier U, Otterbach F, et al. New insight into the SDF-1/CXCR4 axis in a breast carcinoma model: hypoxia-induced endothelial SDF-1 and tumor cell CXCR4 are required for tumor cell intravasation. Mol Cancer Res 2012;10:1021-31.
7. Liao A, Shi R, Jiang Y, et al. SDF-1/CXCR4 axis regulates cell cycle progression and epithelial-mesenchymal transition via up-regulation of survivin in glioblastoma.

Mol Neurobiol 2016;53:210-5.
8. Teng F, Tian WY, Wang YM, et al. Cancer-associated fibroblasts promote the progression of endometrial cancer via the SDF-1/CXCR4 axis. J Hematol Oncol 2016;9:8.
9. Zgraggen S, Huggenberger R, Kerl K, et al. An important role of the SDF-1/CXCR4 axis in chronic skin inflammation. PLoS One 2014;9:e93665.
10. Platt D, Amara S, Mehta T, et al. Violacein inhibits matrix metalloproteinase mediated CXCR4 expression: potential anti-tumor effect in cancer invasion and metastasis. Biochem Biophys Res Commun 2014;455:107-12.
11. Amara S, Chaar I, Khiari M, et al. Stromal cell derived factor-1 and CXCR4 expression in colorectal cancer promote liver metastasis. Cancer Biomark 2015;15:869-79.
12. Shen PF, Chen XQ, Liao YC, et al. MicroRNA-494-3p targets CXCR4 to suppress the proliferation, invasion, and migration of prostate cancer. Prostate 2014;74:756-67.
13. Li Y, Chen M, Yuan J, et al. CXCR4 expression in bladder transitional cell carcinoma and its relationship with clinicopathological features. Urol Int 2014;92:157-63.
14. Liu K, Bao C, Yao N, et al. Expression of CXCR4 and non-small cell lung cancer prognosis: a meta-analysis. Int J Clin Exp Med 2015;8:7435-45.
15. Wang H, Xie F, Hu Z, et al. Elevated expression of CXCR4 and correlation with clinicopathological features and prognosis of non-small cell lung cancer patients: a meta-analysis. Genet Mol Res 2015;14:17893-903.
16. Huang TH, Chiu YH, Chan YL, et al. Prophylactic administration of fucoidan represses cancer metastasis by inhibiting vascular endothelial growth factor (VEGF) and matrix metalloproteinases (MMPs) in Lewis tumor-bearing mice. Mar Drugs 2015;13:1882-900.
17. Gilcy GK, Kuttan G. Evaluation of antiangiogenic efficacy of emilia sonchifolia (L.) DC on tumor-specific neovessel formation by regulating MMPs, VEGF, and proinflammatory cytokines. Integr Cancer Ther 2016;15:NP1-12.
18. Fukunaga S, Maeda K, Noda E, et al. Association between expression of vascular endothelial growth factor C, chemokine receptor CXCR4 and lymph node metastasis in colorectal cancer. Oncology 2006;71:204-11.
19. Zhang R, Pan X, Huang Z, et al. Osteopontin enhances the expression and activity of MMP-2 via the SDF-1/CXCR4 axis in hepatocellular carcinoma cell lines. PLoS One 2011;6:e23831.
20. Fullár A, Dudás J, Oláh L, et al. Remodeling of extracellular matrix by normal and tumor-associated fibroblasts promotes cervical cancer progression. BMC Cancer 2015;15:256.
21. Sung BH, Weaver AM. Exosome secretion promotes chemotaxis of cancer cells. Cell Adh Migr 2017;11:187-95.
22. Li L, Wu S, Li P, et al. Hypoxic preconditioning combined with microbubble-mediated ultrasound effect on MSCs promote SDF-1/CXCR4 expression and its migration ability: an in vitro study. Cell Biochem Biophys 2015;73:749-57.
23. Justus CR, Leffler N, Ruiz-Echevarria M, et al. In vitro cell migration and invasion assays. J Vis Exp 2014.
24. Cavallaro S. CXCR4/CXCL12 in non-small-cell lung cancer metastasis to the brain. Int J Mol Sci 2013;14:1713-27.
25. Li Q, Zhang A, Tao C, et al. The role of SDF-1-CXCR4/CXCR7 axis in biological behaviors of adipose tissue-derived mesenchymal stem cells in vitro. Biochem Biophys Res Commun 2013;441:675-80.
26. Jung MJ, Rho JK, Kim YM, et al. Upregulation of CXCR4 is functionally crucial for maintenance of stemness in drug-resistant non-small cell lung cancer cells. Oncogene 2013;32:209-21.
27. Nakanishi Y, Mizuno H, Sase H, et al. ERK signal suppression and sensitivity to CH5183284/Debio 1347, a selective FGFR inhibitor. Mol Cancer Ther 2015;14:2831-9.
28. Guo F, Wang Y, Liu J, et al. CXCL12/CXCR4: a symbiotic bridge linking cancer cells and their stromal neighbors in oncogenic communication networks. Oncogene 2016;35:816-26.
29. Bleul CC, Fuhlbrigge RC, Casasnovas JM, et al. A highly efficacious lymphocyte chemoattractant, stromal cell-derived factor 1 (SDF-1). J Exp Med 1996;184:1101-9.

Cite this article as: Zeng Y, Wang X, Yin B, Xia G, Shen Z, Gu W, Wu M. Role of the stromal cell derived factor-1/CXC chemokine receptor 4 axis in the invasion and metastasis of lung cancer and mechanism. J Thorac Dis 2017;9(12):4947-4959. doi: 10.21037/jtd.2017.10.138

